Iğdır Üniversitesi Fen Bilimleri Enstitüsü Dergisi, 14(4), 1590-1601, 2024
Journal of the Institute of Science and Technology, 14(4), 1590-1601, 2024

ISSN: 2146-0574, eISSN: 2536-4618

Civil Engineering **DOI: 10.21597/jist.1521794**

Research Article

Received: 24.07.2024 **Accepted: 21.08.2024**

To Cite: Solak, K. & Orhan, S. N. (2024). Comparative Study of Progressive Collapse Behavior of Auxetic Concrete Cellular Structures Under Low-Velocity Impact Loading. *Journal of the Institute of Science and Technology*, 14(4), 1590-1601.

Comparative Study of Progressive Collapse Behavior of Auxetic Concrete Cellular Structures Under Low-Velocity Impact Loading

Kemal SOLAK[1], Süleyman Nazif ORHAN[1*]

Highlights:

- Traditional and stiffened auxetic concrete cellular structures were modeled.
- FE simulations of auxetics were conducted using ANSYS/LS-DYNA under low-velocity impact loading.
- Impact responses of cellular structures were determined.

Keywords:

- Auxetic concrete cellular structures
- Negative Poisson's ratio
- CSCM concrete model
- Numerical simulation
- Low-velocity impact

ABSTRACT:

The combination of auxetic behavior with concrete offers promising advancements in structural materials, providing unique mechanical properties that enhance impact resistance and energy absorption. The study investigates the mechanical behavior of auxetic concrete cellular structures, focusing on elliptic and peanut-shaped unit cells as well as their modified stiffener configurations, under low-velocity impact loading. To compare their impact performance, traditional and stiffened models were analyzed numerically using finite element solver ANSYS/LS-DYNA. The findings indicate significant differences between traditional and stiffened models. Stiffened models, such as SEC and SPC, exhibit higher maximum impact forces compared to traditional models like TEC and TPC. The introduction of stiffeners delays the zero-force phenomenon, resulting in extended energy absorption periods. The TPC model absorbed the most significant proportion of the initial impact velocity among traditional models, whereas the SPC model exhibited the highest energy absorption in models with stiffeners. The study highlights the potential of stiffened auxetic concrete cellular structures to enhance impact resistance and energy dissipation, making them advantageous for applications requiring high structural resilience. Further research into varying impact velocities and loading directions is recommended to optimize these structures for diverse conditions.

[1] Kemal SOLAK (**Orcid ID:** 0000-0001-6957-2689), Süleyman Nazif ORHAN (**Orcid ID:** 0000-0002-1357-6039), Erzurum Technical University, Faculty of Engineering and Architecture, Civil Engineering Department, Erzurum, Türkiye.

***Corresponding Author:** Süleyman Nazif ORHAN, e-mail: s.orhan@erzurum.edu.tr

INTRODUCTION

Recent developments in construction materials have been marked by a shift towards sustainability, enhanced performance, and the integration of advanced technologies. Innovations such as high-performance concrete and self-healing materials are transforming the industry and addressing structural demands (Asgharpour & Hosseini, 2024). Among these advancements, cementitious materials remain a staple due to their versatility, cost-effectiveness, and ease of production (Rosewitz et al., 2019; Xu & Šavija, 2021). Despite their exceptional compressive strength, cementitious materials are inherently brittle and have a low tensile strength, leading to minimal energy absorption and sudden fractures when their tensile limits are exceeded. Consequently, they are unsuitable for applications requiring high energy absorption, such as vibration and impact resistance (Rosewitz et al., 2019; Momoh et al., 2024). However, advancements in manufacturing technologies offer new opportunities to improve the mechanical properties of cement-based materials. The advent of additive manufacturing, or 3D printing, has opened new horizons for producing cement-based materials, offering unprecedented design flexibility and precision (Mobarak et al., 2023; Xie et al., 2024). Additive manufacturing allows for the creation of complex geometries and tailored material properties that are difficult or impossible to achieve with conventional manufacturing techniques (Jiang & Koike, 2023; Zhou et al., 2024). This technology is particularly advantageous for producing engineered cementitious composites (ECC), which exhibit superior mechanical behaviors compared to traditional concrete (Hung et al., 2013; Felekoğlu et al., 2014; Li et al., 2020; Xie et al., 2024). These composites are designed with a micromechanically guided approach, and their enhanced performance is primarily attributed to their unique composition, which typically includes a mix of fine aggregates, cement, water, and randomly distributed short fibers. These fibers bridge microcracks as they form, preventing the localization of stress and the propagation of cracks. This mechanism allows ECC to exhibit strain-hardening behavior and sustain multiple microcracks under tensile loading, each of which can open without leading to catastrophic failure. Thus, ECC exhibits high tensile strength and ductility, even at low fiber levels (Li, 2003; Yang et al., 2007).

On the other hand, auxetic materials, known for their unique property of negative Poisson's ratio, have recently gained significant attention in civil engineering. In contrast to cementitious materials, auxetics offer substantial advantages, including enhanced energy absorption and higher shear and fracture resistance (Orhan & Erden, 2022a, 2022b; Momoh et al., 2024). Consequently, another approach to enhance the insufficient mechanical properties of conventional cement-based materials is incorporating auxetic metamaterials in cementitious composites (Zhou et al., 2020; Luo et al., 2022; Tzortzinis et al., 2022; Zhong et al., 2022; Chen et al., 2023; Xu et al., 2024; Xu & Šavija, 2024). In a study conducted by Zhong et al. (2022), the mechanical properties of auxetic cementitious composites designed using single and layered re-entrant aluminum frames were compared. The composites' compressive strength and energy absorption capacity were determined through experiments and finite element analysis, and it was found that the layered composite showed better mechanical performance. Luo et al. (2022) examined the axial compressive performance of a novel tubular composite designed using an auxetic steel tube and concrete. The mechanical behavior of this tubular structure was compared with composites, including tubes that do not show auxetic behavior. As a result of the experiments and finite element analyzes, it was determined that the use of auxetic tubes created a better confinement effect on the concrete. Chen et al. (2023) experimentally examined the compressive behavior of the composite structures manufactured using polylactic acid auxetic lattices (re-entrant, octet, and triangular) and ultra-high performance concrete (UHPC) under static and dynamic effects.

The results were compared with the plain and steel fiber-reinforced ultra-high performance concrete, and the re-entrant lattice was found to be the most suitable structure for composites produced with UHPC. Xu et al. (2024) designed an original auxetic cementitious composite structure consisting of a 3D printed auxetic frame and cementitious mortar as filler. The mechanical properties of this composite were examined under uniaxial compression and cyclic loading. As a result of the experiments and numerical analysis, it was determined that this composite structure has a higher energy absorption ability compared to conventional cementitious mortar and the polymeric auxetic frame. Xu and Sajiva (2024) produced composite structures using four different polymeric auxetic frames (re-entrant, rotating-square, chiral, and missing rib) and cementitious mortar. The compressive behavior of these composite structures was examined both numerically and experimentally. In conclusion, all structures were found to have higher energy absorption and ductility than the traditional mortar.

In addition to the use of concrete and auxetic structures in composite forms, as mentioned above, recent studies have focused on designing cellular cementitious composites to exhibit auxetic behavior and determining their mechanical properties under different loading conditions (Xu et al., 2020; Xu et al., 2021; Lyngdoh et al., 2022; Chen et al., 2024; Xie et al., 2024). Among these studies, Xu et al. (2020) designed and investigated the mechanical behavior of cementitious cellular auxetic composites with elliptically-shaped unit cells and various fiber contents under uniaxial compression and cyclic loading. Experimental studies on samples produced using 3D printing techniques revealed that the energy absorption capabilities of these composites are promising for engineering applications. Xu et al. (2021) modeled and produced cementitious cellular composites with three different unit cell shapes utilizing 3D printing technology. The behavior of these composites under compression and different boundary conditions was investigated experimentally and numerically. It was found that two of these composites exhibited auxetic behavior and were suitable for various civil engineering applications due to their high energy absorption capacities. Chen et al. (2024) designed three different cementitious cellular composites with elliptical, re-entrant, and chiral unit cells and studied their mechanical performance under flexural and compressive effects. Experiments and numerical analyzes indicated that these structures exhibited auxetic behavior under compression, while this behavior was not observed under bending. Among the structures examined, the composite with elliptically shaped unit cells demonstrated the best results regarding strength and energy absorption capacity. Xie et al. (2024) modeled two peanut-shaped cementitious cellular composites with different unit cell geometries. The mechanical properties of these structures under compression were determined and compared with elliptically-shaped cementitious cellular composites, experimentally and numerically. As a result, peanut-shaped composites were found to have better auxetic behavior and higher energy absorption capacity than elliptically-shaped ones.

In this paper, the mechanical behavior of auxetic concrete cellular structures is examined, with a focus on elliptic and peanut-shaped unit cells and their modified stiffener configurations under low-velocity impact loading. To assess their impact performance, both traditional and stiffened models were analyzed using the finite element (FE) solver ANSYS/LS-DYNA. This study is expected to provide valuable insights for civil engineering applications where impact resistance and energy dissipation are essential.

MATERIALS AND METHODS

LS-DYNA Concrete Material Model

In recent decades, numerous material models have been developed to describe the behavior of concrete and similar materials under different loading conditions, such as quasi-static loading, low/high-velocity impacts, and shock/blast loads. LS-DYNA offers a variety of concrete constitutive models such as Karagozian and Case (*Mat_Concrete_Damage/MAT_072), Winfrith (*Mat_Winfrith_Concrete/MAT_084), Continuous Surface Cap (*Mat_CSCM_Concrete/MAT_159) and Holmquist-Johnson Cook (*Mat_Johson_Holmquist_Concrete/MAT_111), which are frequently used in the literature (Abedini & Zhang, 2021). The aforementioned models offer distinct benefits, with simple keyword inputs and automatic parameter generation versions provided by each.

Continuous Surface Cap Model (CSCM) in LS-DYNA, a widely adopted nonlinear concrete model, has been validated and applied in studies involving blast response of concrete walls (Yan et al., 2016), rock cutting simulations (Stopka, 2021), and low-velocity impact response of cementitious composites (Yin et al., 2023). CSCM is a visco-elastic-plastic model for concrete that effectively captures a range of material properties, such as damage-induced softening, modulus reduction, shear dilation, shear compaction, confinement effects, and strain rate dependent, as seen in Figure 1 (Abdelwahed et al., 2015; Weng et al., 2020). CSCM employs a cap formulation to characterize the compaction behavior of the concrete. Furthermore, a depiction of the yield surface is presented in Figure 2, illustrating shear strength plotted against pressure axes. Stress in the concrete is recalculated and updated during each time step of the analysis. The concrete behaves elastically if the calculated stress is within or on the yield surface. If the stress exceeds the yield surface, a plasticity algorithm returns the stress state to the yield surface. The model derives default parameters from unconfined compression strength, aggregate size, and units, calibrated using data ranging from 20 to 58 MPa for unconfined compressive strength and aggregate sizes of 8 to 24 mm (Murray, 2004). In this study, CSCM model parameters were derived based on a concrete unconfined compressive strength of 30 MPa and an aggregate size of 8 mm, as listed in Table 1.

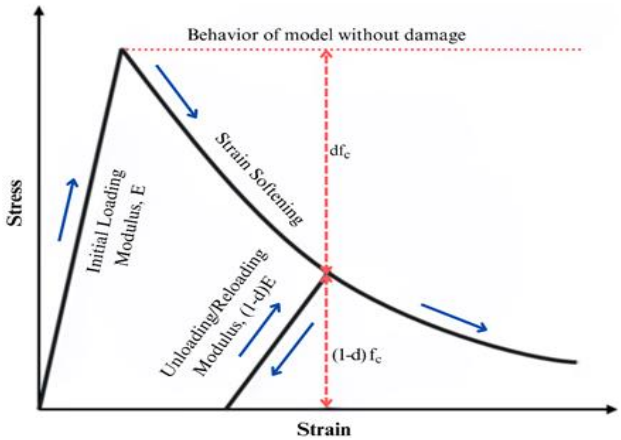

Figure 1. Characteristics of strain softening and modulus reduction of CSCM model (Murray, 2007)

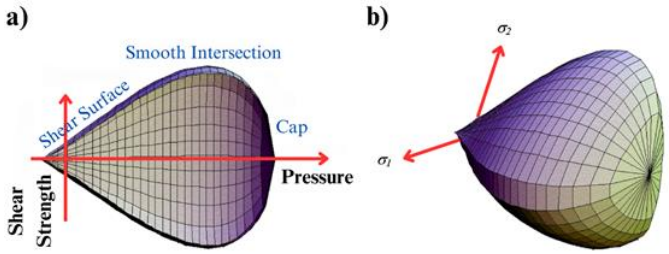

Figure 2. Yield surface of CSCM in two (a) and three (b) dimensions (Murray, 2007)

Table 1. Parameters of CSCM model used in FE simulation (Units are in GPa, kg, mm, ms)

Parameters	Values	Parameters	Values
RO	$2.4x10^{-6}$	BETA2	70.57
NPLOT	1	R	5
INCRE	$1.741x10^{-5}$	X0	0.09054
IRATE	1	W	0.05
ERODE	1.1	D1	0.25
RECOV	0.1	D2	0.3492
ITRETRC	0	B	100
PRED	0	GFC	0.005392
G	11.46	D	0.1
K	12.55	GFT	$5.392x10^{-5}$
ALPHA	0.0145	GFS	$5.392x10^{-5}$
THETA	0.2965	PWRC	5
LAMDA	0.01051	PWRT	1
BETA	19.29	PMOD	0
NH	1	ETA0C	$4.587x10^{-4}$
CH	0	NC	0.78
ALPHA1	0.7473	ETA0T	0.002242
THETA1	1.151	NT	0.48
LAMDA1	0.17	OVERC	0.02145
BETA1	70.57	OVERT	0.02145
ALPHA2	0.66	SRATE	1
THETA2	1.387	REPOW	1
LAMDA2	0.16		

Design of Auxetic Concrete Cellular Structures

Numerous unit cells have been proposed and investigated in the literature to achieve auxetic behavior in structures. In this study, auxetic cellular structures were developed using two different auxetic unit cells, along with modified versions that included stiffeners at the perforation centers. The designs of the elliptic and peanut-shaped perforations were based on our previous studies (Solak & Orhan, 2022, 2023, 2024). The computer-aided design (CAD) models were carefully created using SolidWorks 2019 (Dassault Systems, Massachusetts, USA) software, ensuring the desired characteristics of each shape were accurately represented. The geometric details of the auxetic unit cells are provided in Table 2. The unit cell design utilized the following geometric parameters: side length (L), large circle radius (R), small circle radius (r), stiffener thickness (t), long side length of perforations or stiffener length (s), and short side length of perforations (d). Each auxetic cellular structure was created with dimensions of 200x200 mm and a thickness of 50 mm. A planar form with a 4x4 array layout was constructed using the auxetic unit cells and then extruded to achieve the desired thickness, as illustrated in Figure 3. To differentiate between the auxetic structures analyzed for their mechanical properties and to facilitate comparison of the results, the following abbreviations were used: TEC for traditional elliptic-shaped concrete cellular structure, SEC for stiffened elliptic-shaped

concrete cellular structure, TPC for traditional peanut-shaped concrete cellular structure, and SPC for stiffened peanut-shaped concrete cellular structure.

Table 2. Geometric details of auxetic unit cells

Unit cells	L (mm)	s (mm)	d (mm)	R (mm)	r (mm)	t (mm)
Traditional elliptic perforation	50	28	12	-	-	-
Traditional peanut perforation	50	28	-	8	6	-
Stiffened elliptic perforation	50	28	12	-	-	2.6
Stiffened peanut perforation	50	28	-	8	6	2.6

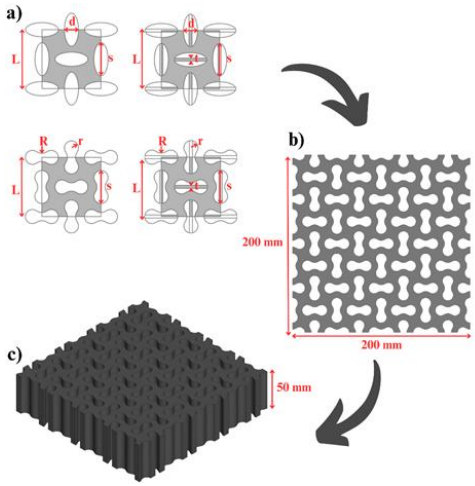

Figure 3. Auxetic structures design methodology: (a) auxetic unit cells, (b) planar form, (c) cellular form

Finite Element Analysis (FEA) Setup and Verification

A numerical model was developed using ANSYS/LS-DYNA (Ansys Inc., PA, USA) finite element software to investigate the progressive collapse behavior of auxetic concrete cellular structures under low-velocity impact. This model comprises three main components: impactor, auxetic cellular structure, and lower plate. The impactor is constrained in all rotations and translations except for its movement along the loading axis. The impactor contacts the auxetic cellular structure, positioned on the fixed lower plate, with a specified initial velocity. The fixed lower plate and the impactor are designed with a diameter of 300 mm and a thickness of 30 mm. The impactor is assumed to reach a velocity of 7.5 m/s at the initial contact, and this initial velocity is applied consistently across all numerical models. For numerical modeling of the impactor and fixed lower plate, a non-deforming material identified as *MAT_RIGID was employed, featuring a density of 7850 kg/m³, Young's modulus of 210 GPa, and a Poisson's ratio of 0.3. Furthermore, auxetic concrete cellular structures were modeled using the *MAT_CSCM, as mentioned above. The initial velocity along the loading axis of the impactor is specified using *INITIAL_VELOCITY_GENERATION. In the analysis, *CONTACT_ERODING_SINGLE_SURFACE was utilized to model the interaction between the concrete and the plates. This contact method is recommended when solid elements involved in contact definitions may erode due to specified material failure criteria (Anonymous, 2016). Static and dynamic friction coefficients were also set to 0.25 (Luo et al., 2022). Reaction forces during impact were computed from the impactor using *FORCE_TRANSDUCER. Figure 4 depicts the finite element model, showing boundary conditions and LS-DYNA cards.

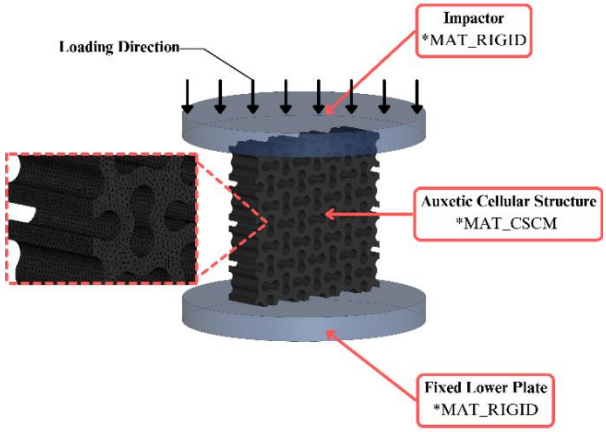

Figure 4. The finite element model including boundary conditions, mesh discretization, and LS-DYNA cards

The tetrahedral solid elements with four nodes were used to mesh the auxetic cellular structures, ensuring precise representation of intricate curves and edges, considering previous studies (Gürbüz & Kocaman, 2024; Kocaman & Gürbüz, 2024; Orhan & Alkan, 2024). A mesh convergence study is conducted using the TEC model to assess the accuracy of the analyzes. Various numerical models were created with different mesh sizes (0.5 mm, 1 mm, 2 mm, 4 mm, 5 mm) and compared based on peak impact force. After multiple trials, a mesh size of 2 mm was chosen for all models as the optimal option, effectively balancing computational efficiency with precision requirements. The results of the mesh convergence study are given in Figure 5.

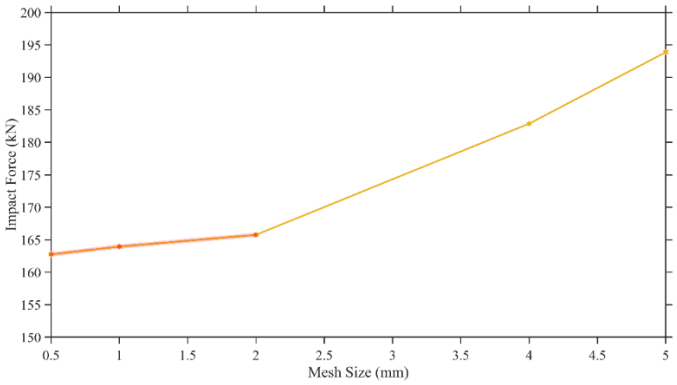

Figure 5. The results of the mesh convergence study

RESULTS AND DISCUSSION

Figure 6-9 illustrates the mechanical behavior of concrete cellular structures with elliptic and peanut perforations under low-velocity impact loading. The time history of impact force curves corresponding to 5 ms analysis time is given in Figure 6. The traditional auxetic models, TEC and TPC, exhibited nearly identical maximum impact forces of 165.75 kN and 163.89 kN, respectively. Furthermore, the stiffened models, SEC and SPC, had maximum impact forces of approximately 193.31 kN and 191.52 kN, respectively. When comparing the traditional and stiffened models among themselves, it is evident that although they have similar maximum impact forces, each model displays a distinct force trend after 0.3 ms, as seen in Figure 6-7. After the TEC model reaches its peak impact force, the force trend approaches zero at 0.3 ms. When a stiffener is added to the elliptic model, the SEC model reaches zero force at 0.45 ms. The TPC model reaches zero force at 0.6 ms, and the SPC model does so at 0.7 ms. This indicates that traditional models reach zero force sooner than stiffened models. The introduction of stiffeners to cellular structures delays the zero-force phenomenon, allowing the structures to absorb more energy. Additionally, while the impact force curve remained

constant in the TEC and SEC models, fluctuations were observed in the force curves of the TPC and SPC models. These fluctuations indicate the occurrence of progressive damage. After 4 ms, all models exhibited a force curve approaching zero. Figure 8 presents the deformation trends of auxetic concrete cellular structures along with their corresponding damage ratios. Auxetic models with elliptic and peanut perforations consist of solid blocks (Wang et al, 2020). Under axial loading, these structures absorb the applied load by rotating the solid blocks. The most noticeable rotational deformation is seen in the TEC and SEC models, while a slight rotational deformation is observed in the TPC and SPC models. In all models, initial fractures began at the junction points of the solid blocks. This type of deformation in concrete-based cellular auxetics is consistent with findings reported in several studies in the literature (Xu et al., 2020, 2021). Additionally, as the impactor hit the auxetic structures at a speed of 7.5 m/s, the deformation progressed from the top to the bottom of the structures.

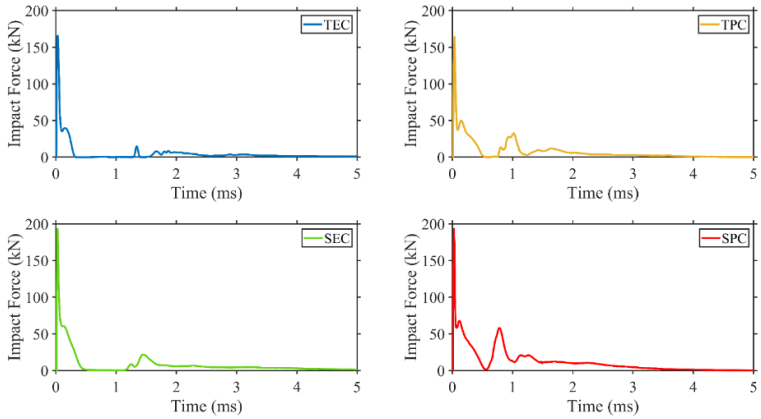

Figure 6. Time history of impact force for 5 ms period

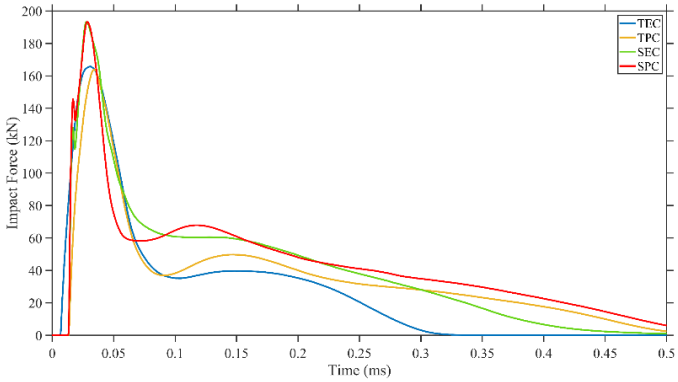

Figure 7. Time history of impact force for 0.5 ms period

Figure 9 shows the time history of the velocity curve of the rigid impactor during the 5 ms analysis period. Additionally, the results for the auxetic concrete cellular structures are also provided in Table 3. The impactor, initially striking the auxetic structures at 7.5 m/s, reached final velocities of 6.02 m/s in the TEC model, 5.23 m/s in the TPC model, 5.14 m/s in the SEC model, and 3.98 m/s in the SPC model at the end of the analysis. Additionally, the impactor displaced 31.9 mm along the loading axis in the TEC model, 28.4 mm in the TPC model, 28.7 mm in the SEC model, and 23.7 mm in the SPC model. The absorbed energy ratio value in Table 3 is calculated as the percentage ratio of the impactor final velocity to the initial velocity. Among traditional models, the TPC model absorbed the most impactor energy, with a ratio of 30.27%. Among stiffened models, the SPC model absorbed the most impactor energy, with a ratio of 46.94%. In dynamic impact analysis, a lower peak force is desirable (Ha & Lu, 2020). As shown in Table 3, while the TEC and TPC models had nearly identical

maximum impact forces, the TPC model absorbed more energy, giving it an advantage over the TEC model. A similar scenario is observed in models with stiffeners. Although the SPC and SEC models have identical maximum impact force, the SPC model is more advantageous in terms of velocity absorbing. Additionally, the introduction of the stiffener to the models enhances the energy absorption capability of the SEC and SPC models compared to their traditional counterparts.

Table 3. The results of low-velocity impact analysis

Specimen	Maximum impact force (kN)	Impactor initial velocity (m/s)	Impactor final velocity (m/s)	Absorbed energy ratio (%)	Impactor total displacement (mm)
TEC	165.75	7.5	6.02	19.73	31.9
TPC	163.89	7.5	5.23	30.27	28.4
SEC	193.31	7.5	5.14	31.47	28.7
SPC	191.52	7.5	3.98	46.94	23.7

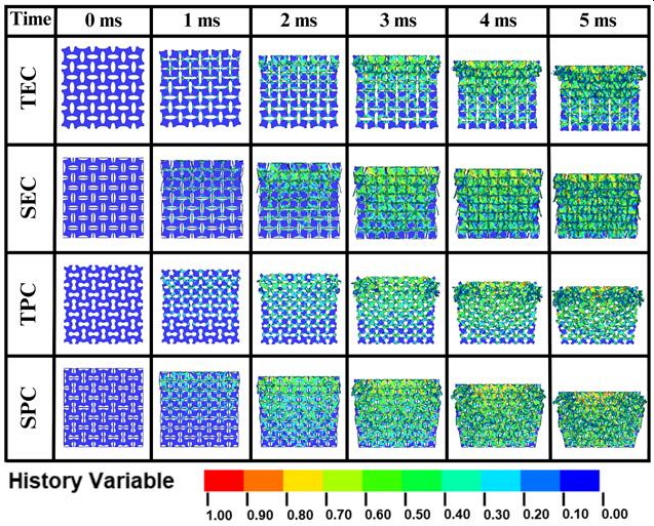

Figure 8. Deformation mechanism of auxetic concrete cellular structures

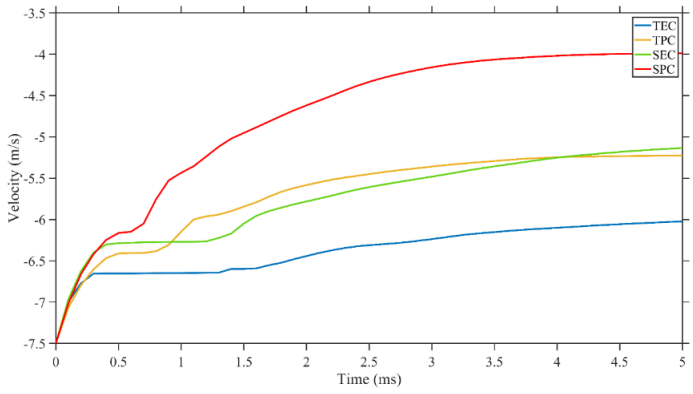

Figure 9. Time history of velocity

CONCLUSION

In this study, the mechanical behaviors of auxetic concrete cellular structures with elliptic and peanut perforations, along with their modified versions featuring added stiffeners, were investigated numerically under low-velocity impact loading. A thorough examination of auxetic concrete cellular structures has revealed several key findings, highlighting their importance in civil engineering applications.

• The mechanical behavior of concrete cellular structures with elliptic and peanut perforations under low-velocity impact loading shows distinct differences between traditional and stiffened models.

• Traditional models (TEC, TPC) demonstrated identical maximum impact force, whereas stiffened models (SEC, SPC) also exhibited similar maximum impact force.

• Among traditional models, the TPC model absorbed the most significant proportion of the initial impact velocity, while the SPC model exhibited the highest energy absorption in models with stiffeners.

• The addition of stiffeners in the SEC and SPC models increases the maximum impact forces and delays the zero-force phenomenon, thereby enhancing energy absorption compared to traditional counterparts.

The study highlights the significant advantages of incorporating stiffeners into auxetic concrete cellular structures, demonstrating their potential to improve impact resistance and energy absorption. These findings suggest that stiffened auxetic concrete cellular structures offer valuable benefits for applications requiring high energy dissipation levels and enhanced structural performance. Additionally, the impact velocities, loading directions and auxetic unit cells explored were limited, and further studies with varying conditions could provide a more comprehensive understanding of auxetic concrete cellular structures. Exploring these aspects in future research could lead to optimized designs and broaden the applicability of auxetic concrete cellular structures in diverse civil engineering applications.

Conflict of Interest

The article authors declare that there is no conflict of interest between them.

Author's Contributions

The authors declare that they have contributed equally to the article.

REFERENCES

Abdelwahed, B., Belkassem, B., Pyl, L., & Vantomme, J. (2015). Behaviour of reinforced concrete knee beam-column joint in case of ground corner column loss-numerical analysis. In: COMPDYN 2015 - 5th ECCOMAS Thematic Conference on Computational Methods in Structural Dynamics and Earthquake Engineering. Crete Island, Greece.

Abedini, M., & Zhang, C. (2021). Performance Assessment of Concrete and Steel Material Models in LS-DYNA for Enhanced Numerical Simulation, A State of the Art Review. Archives of Computational Methods in Engineering, 28(4), 2921–2942.

Anonymous, (2016). LS-DYNA Keyword User's Manual Ver. 971. Livermore Software Technology Corporation, California, USA.

Asgharpour, F., & Hosseini, M. (2024). Advancements and Challenges in the Development of self-healing Concrete for Sustainable Construction-A Critical Review. Alpha Journal of Engineering and Applied Sciences, 2(1), 33 – 48.

Chen, M., Chen, Z., Xuan, Y., Zhang, T., & Zhang, M. (2023). Static and dynamic compressive behaviour of 3D printed auxetic lattice reinforced ultra-high performance concrete. Cement and Concrete Composites, 139, 105046.

Chen, M., Fang, S., Wang, G., Xuan, Y., Gao, D., & Zhang, M. (2024). Compressive and flexural behaviour of engineered cementitious composites based auxetic structures: An experimental and numerical study. Journal of Building Engineering, 86, 108999.

Felekoğlu, K., Felekoğlu, B., Ranade, R., Lee, B. Y., & Li, V. C. (2014). The role of flaw size and fiber distribution on tensile ductility of PVA-ECC. Composites Part B: Engineering, 56, 536 - 545.

Gürbüz, M., & Kocaman, İ. (2024). Enhancing seismic resilience: A proposed reinforcement technique for historical minarets. Engineering Failure Analysis, 156, 107832.

Ha, N. S., & Lu, G. (2020). A review of recent research on bio-inspired structures and materials for energy absorption applications. Composites Part B: Engineering, 181, 107496.

Hung, C. C., Su, Y. F., & Yu, K. H. (2013). Modeling the shear hysteretic response for high performance fiber reinforced cementitious composites. Construction and Building Materials, 41.

Jiang, X., & Koike, R. (2023). High gravity material extrusion system and extruded polylactic acid performance enhancement. Scientific Reports, 13, 14224.

Kocaman, İ., & Gürbüz, M. (2024). Enhancing seismic performance of historic mosques through retrofitting measures. Engineering Structures, 301, 117245.

Li, V. C. (2003). On engineered cementitious composites (ECC), A review of the material and its applications. Journal of Advanced Concrete Technology, 1(3), 215-230.

Li, V. C., Bos, F. P., Yu, K., McGee, W., Ng, T. Y., Figueiredo, S. C., Nefs, K., Mechtcherine, V., Nerella, V. N., Pan, J., Zijl, G., & Kruger, P. J. (2020). On the emergence of 3D printable Engineered, Strain Hardening Cementitious Composites (ECC/SHCC). Cement and Concrete Research, 132, 106038.

Luo, C., Ren, X., Han, D., Zhang, X. G., Zhong, R., Zhang, X. Y., & Xie, Y. M. (2022). A novel concrete-filled auxetic tube composite structure: Design and compressive characteristic study. Engineering Structures, 268, 114759.

Lyngdoh, G. A., Kelter, N. K., Doner, S., Krishnan, N. M. A., & Das, S. (2022). Elucidating the auxetic behavior of cementitious cellular composites using finite element analysis and interpretable machine learning. Materials and Design, 213, 110341.

Mobarak, M. H., Islam, M. A., Hossain, N., Al Mahmud, M. Z., Rayhan, M. T., Nishi, N. J., & Chowdhury, M. A. (2023). Recent advances of additive manufacturing in implant fabrication - A review. Applied Surface Science Advances, 18, 100462.

Momoh, E. O., Jayasinghe, A., Hajsadeghi, M., Vinai, R., Evans, K. E., Kripakaran, P., & Orr, J. (2024). A state-of-the-art review on the application of auxetic materials in cementitious composites. Thin-Walled Structures, 196, 111447.

Murray, Y. (2007). Users Manual for LS-DYNA Concrete Material Model 159. Technical report, Federal Highway Administration, Virginia, USA.

Murray, Y. D. (2004). Theory and evaluation of concrete material model 159. In 8th International LS-DYNA Users Conference, Detroit, USA.

Orhan, S. N., & Alkan, E. (2024). Rigid fixation of the sternum: a comparative biomechanical study. Journal of the Brazilian Society of Mechanical Sciences and Engineering, 46(6), 1–9.

Orhan, S. N., & Erden, Ş. (2022a). Design and finite element analysis of a novel auxetic structure. Challenge Journal of Structural Mechanics, 8(4), 159 - 165.

Orhan, S. N., & Erden, Ş. (2022b). Numerical investigation of the mechanical properties of 2D and 3D auxetic structures. Smart Materials and Structures, 31, 065011.

Rosewitz, J. A., Choshali, H. A., & Rahbar, N. (2019). Bioinspired design of architected cement-polymer composites. Cement and Concrete Composites, 96, 252 - 265.

Solak, K., & Orhan, S. N. (2022). Performance evaluation of peanut-shaped tubular auxetics with enhanced stiffness: a finite element study. Modelling and Simulation in Materials Science and Engineering, 31, 015006.

Solak, K., & Orhan, S. N. (2023). Axial compression behaviour of concrete-filled auxetic tubular short columns. Challenge Journal of Concrete Research Letters, 14(1), 1 - 9.

Solak, K., & Orhan, S. N. (2024). Quasi-static crashworthiness behaviour of auxetic tubular structures based on rotating deformation mechanism. Smart Materials and Structures, 33, 055016.

Stopka, G. (2021). Modelling of Rock Cutting with Asymmetrical Disc Tool Using Discrete-Element Method (DEM). Rock Mechanics and Rock Engineering, 54, 6265 - 6279.

Tzortzinis, G., Gross, A., & Gerasimidis, S. (2022). Auxetic boosting of confinement in mortar by 3D reentrant truss lattices for next generation steel reinforced concrete members. Extreme Mechanics Letters, 52, 101681.

Wang, H., Zhang, Y., Lin, W., & Qin, Q. H. (2020). A novel two-dimensional mechanical metamaterial with negative Poisson's ratio. Computational Materials Science, 171, 109232.

Weng, Y. H., Qian, K., Fu, F., & Fang, Q. (2020). Numerical investigation on load redistribution capacity of flat slab substructures to resist progressive collapse. Journal of Building Engineering, 29, 101109.

Xie, J., Xu, Y., Meng, Z., Liang, M., Wan, Z., & Šavija, B. (2024). Peanut shaped auxetic cementitious cellular composite (ACCC). Construction and Building Materials, 419, 135539.

Xu, Y., Meng, Z., Bol, R. J. M., & Šavija, B. (2024). Spring-like behavior of cementitious composite enabled by auxetic hyperelastic frame. International Journal of Mechanical Sciences, 275, 109364.

Xu, Y., & Šavija, B. (2021). Architected Cementitious Cellular Materials: Peculiarities and opportunities. Heron, 66(2–3).

Xu, Y., & Šavija, B. (2024). Auxetic cementitious composites (ACCs) with excellent compressive ductility: Experiments and modeling. Materials & Design, 237, 112572.

Xu, Y., Schlangen, E., Luković, M., & Šavija, B. (2021). Tunable mechanical behavior of auxetic cementitious cellular composites (CCCs): Experiments and simulations. Construction and Building Materials, 266, 121388.

Xu, Y., Zhang, H., Schlangen, E., Luković, M., & Šavija, B. (2020). Cementitious cellular composites with auxetic behavior. Cement and Concrete Composites, 111, 103624.

Yan, D., Yin, H., Wu, C., Li, Y., Baird, J., & Chen, G. (2016). Blast response of full-size concrete walls with chemically reactive enamel (CRE)-coated steel reinforcement. Journal of Zhejiang University: Science A, 17, 689-701.

Yang, E. H., Yang, Y., & Li, V. C. (2007). Use of high volumes of fly ash to improve ECC mechanical properties and material greenness. ACI Materials Journal, 104(6), 620 - 628.

Yin, X., Li, Q., Xu, X., Chen, B., Guo, K., & Xu, S. (2023). Investigation of continuous surface cap model (CSCM) for numerical simulation of strain-hardening fibre-reinforced cementitious composites against low-velocity impacts. Composite Structures, 304(1), 116424.

Zhong, R., Ren, X., Yu Zhang, X., Luo, C., Zhang, Y., & Min Xie, Y. (2022). Mechanical properties of concrete composites with auxetic single and layered honeycomb structures. Construction and Building Materials, 322, 126453.

Zhou, H., Jia, K., Wang, X., Xiong, M. X., & Wang, Y. (2020). Experimental and numerical investigation of low velocity impact response of foam concrete filled auxetic honeycombs. Thin-Walled Structures, 154, 106898.

Zhou, L., Miller, J., Vezza, J., Mayster, M., Raffay, M., Justice, Q., Tamimi, Z. A., Hansotte, G., Sunkara, L. D., & Bernat, J. (2024). Additive Manufacturing: A Comprehensive Review. Sensors, 24(9), 2668.